RESEARCH ARTICLE

High-precision three-dimensional inkjet technology for live cell bioprinting

Daisuke Takagi*, Waka Lin, Takahiko Matsumoto, Hidekazu Yaginuma, Natsuko Hemmi, Shigeo Hatada, Manabu Seo

Ricoh Company Ltd., Healthcare Business Group, Biomedical Business Center, Kawasaki-city, 210-0821, Japan

Abstract: In recent years, bioprinting has emerged as a promising technology for the construction of three-dimensional (3D) tissues to be used in regenerative medicine or *in vitro* screening applications. In the present study, we present the development of an inkjet-based bioprinting system to arrange multiple cells and materials precisely into structurally organized constructs. A novel inkjet printhead has been specially designed for live cell ejection. Droplet formation is powered by piezoelectric membrane vibrations coupled with mixing movements to prevent cell sedimentation at the nozzle. Stable drop-on-demand dispensing and cell viability were validated over an adequately long time to allow the fabrication of 3D tissues. Reliable control of cell number and spatial positioning was demonstrated using two separate suspensions with different cell types printed sequentially. Finally, a process for constructing stratified Mille-Feuille-like 3D structures is proposed by alternately superimposing cell suspensions and hydrogel layers with a controlled vertical resolution. The results show that inkjet technology is effective for both two-dimensional patterning and 3D multilayering and has the potential to facilitate the achievement of live cell bioprinting with an unprecedented level of precision.

Keywords: Drop-on-demand; three-dimensional tissue engineering; drug discovery; regenerative medicine; hydrogel

*Correspondence to: Daisuke Takagi, Ricoh Company Ltd., Healthcare Business Group, Biomedical Business Center, Kawasaki-city, 210-0821, Japan; daisuke.Takagi@jp.ricoh.com

Received: May 14, 2019; **Accepted:** May 27, 2019; **Published Online:** July 1, 2019

Citation: Takagi D, Lin W, Matsumoto T, *et al*., 2019, High-precision three-dimensional inkjet technology for live cell bioprinting. Int J Bioprint, 5(2): 208. http://dx.doi.org/10.18063/ ijb.v5i2.208

1. Introduction

The field of tissue engineering has developed considerably in recent years, along with the increasing interest in regenerative medicine globally. Advances in stem cell research, particularly the discovery of induced pluripotent stem cells[1], have provided a means to culture and manipulate cells from organs, which were once considered impossible to regenerate. *In vitro* production of functional tissue analogs has become a reality, and tissue engineering has numerous potential applications in therapeutic areas including tissue repair and organ replacement, in addition to developing applications for drug discovery, disease modeling, and alternatives for animal testing. Today, one of the major challenges remains how to reproduce three-dimensional (3D) structures of tissues with matching complexity and functionality. The development of novel technologies for biofabrication, particularly bioprinting, has attracted a lot of attention considering their potential to arrange cells and materials into structurally organized constructs[2].

Current bioprinting technologies are based on three major approaches, including inkjet, extrusion, and laser printing methods[3,4]. Extrusion-based strategies are the most extensively developed due to their capacity to develop 3D constructs and networks in a relatively straightforward manner using high viscosity materials that can integrate extracellular matrix (ECM) such as collagen. However, the approach is not suitable since it does not facilitate precise control over the deposition of a small number of cells. Although laser facilitates printing with a very high resolution, its productivity remains limited due to the complexity and cost of the system, in

addition to the requirement for the preparation of ribbons of cells and hydrogels. Conversely, inkjet printing, and more generally, droplet-based bioprinting[5], have great promise as a simple and efficient method for the precise patterning of multiple cell types and bioink components including active biomacromolecules[6], especially since a drop-on-demand control of small volumes down to a few hundred picoliters can be expected. However, inkjet technology has several limitations that impair its further adoption in 3D construction. Although some of the earliest reports of successful bioprinting in the mid-2000s were inkjet based[7-9], few concrete results of fully functional inkjet-produced tissues have been reported to date.

The first notable limitation of inkjet bioprinting is that ejecting large cell-sized particles from common printheads is a challenge. Successful ejection has been reported[10-13], and acoustic ejection achieved in live cell printing[13]; however, cell sedimentation inside the printhead chamber and clogging of the nozzle is expected to rapidly compromise any reliable control of droplet formation over the length of time required to produce a 3D tissue. Second, the range of materials that can be used as substrates to carry the cells is limited to ejectable low-viscosity liquids so that shaping fine 3D structures with suitable mechanical properties is particularly challenging. Various strategies have been reported including coprinting hydrogel precursors with the appropriate cross-linking agent, which facilitates rapid gelation on contact[14-16] or deposition of one liquid into a bath of the other one[17]. However, so far, the results have been generally limited to two-dimensional (2D) cell patterning or roughly shaped 3D cell-laden structures with no spatial positioning at the cellular level.

To address the above challenges, we report here the development of an inkjet bioprinter equipped with a newly designed printhead specially optimized for live cell ejection. For this purpose, we have adapted a bending-type piezoelectric actuator coupled to a simple open head chamber without any narrow flow channel. Such a piezoelectric device has been applied in some previous publications from other groups for continuous cell spraying, but very few studies have reported its application to drop-on-demand cell deposition[18]. The present study integrates the droplet formation and mixing mechanism in our prototype printhead. Stability of cell dispensing and viability is validated over an adequately extended period to facilitate the fabrication of a substantial tissue construct. We then demonstrate the feasibility of building a multi-ink printing system to construct stratified Mille-Feuille-like structures with controlled thickness by alternating cell suspension and hydrogel layers. Therefore, exploiting the full potential of inkjet technology promises to facilitate high-precision multi-ink 3D bioprinting.

2. Materials and Methods

2.1. Cell Cultures

All cells were cultured in a 5% CO_2 incubator at 37.0°C and passaged manually every 2 to 3 days to maintain a subconfluent state. NIH/3T3 mouse fibroblast cell line (clone 5611, JCRB Cell Bank) and normal human dermal fibroblasts (NHDF, CC-2509, Lonza Inc.) were cultured in Dulbecco's Modified Eagle's Medium (Thermo Fisher Scientific Inc.) supplemented with 10% fetal bovine serum (Biowest) and 1% penicillin-streptomycin (26253-84, NACALAI TESQUE, INC). Human umbilical blood vein endothelial cells (HUVEC, CC-2519, Lonza Inc.) were cultured in endothelial cell growth medium (EGM, Lonza Inc.) with supplements as recommended by the manufacturer. For bioink preparation, the cells were washed twice with Dulbecco's phosphate-buffered saline without calcium and magnesium (DPBS, Thermo Fisher Scientific Inc.), detached with 0.05% Trypsin-EDTA (25300054, Thermo Fisher Scientific Inc.), and centrifuged at 400 g for 5 min at 4°C. The cell pellets were re-suspended in fresh DPBS at room temperature and used within 30 min after suspension.

2.2. Inkjet Print Head Development

The cell-printing head in Figure 1A presents an original architecture comprising a chamber holding the cell suspension, a disk membrane (which is fixed at the circumference of the bottom of the chamber), a nozzle with an aperture at the center of the membrane, and an annular piezoelectric actuator fixed outside below the membrane

We were able to perform subsequent experiments with more advanced processes for the spatial positioning of cell-containing droplets by achieving a reliable ejection of living cell.

2.3. Evaluation of Inkjetting Condition

To determine the optimal printing conditions, optical monitoring devices were assembled as follows. Observation of drop formation was carried out with an experimental apparatus with a high-speed camera (HPV-2, Shimadzu Corporation) and a stroboscopic flash lamp (PE60-SG, Panasonic) aligned on a horizontal axis under the printhead nozzle. The chamber was filled with NIH/3T3 suspension with DPBS solution. By applying a signal to the piezoelectric actuator of the cell-printing head, a droplet is ejected from the cell-printing head. The frequency of the applied signal was fixed to the fundamental frequency of the membrane.

2.4. Evaluation of Mixing Condition

Observation of cell suspension mixing was carried out with an experimental apparatus with a ring-type illumination

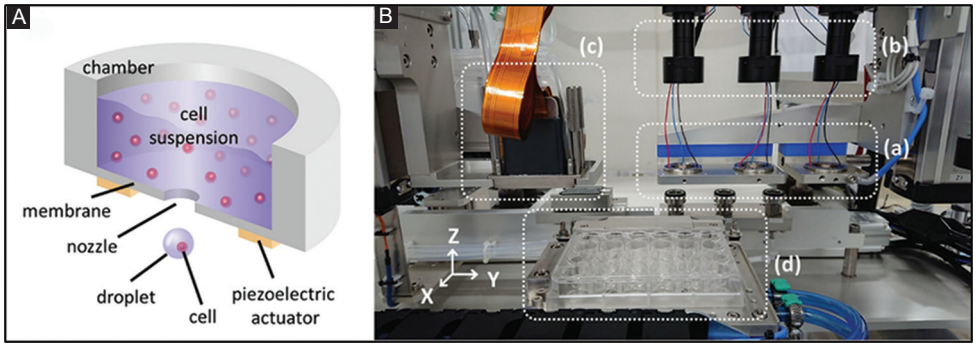

Figure 1. Overview of the inkjet bioprinting system. (**A**) Schematic cross-sectional three-dimensional (3D) view of the cell-printing head. (**B**) Photograph of the 3D bioprinting system setup composed of (a) three cell-printing heads controlled in the X and Z directions, (b) cameras for real-time observation of the mixing state in the inkjet head chambers, (c) two industrial inkjet heads for hydrogel printing controlled in the same directions as (a), and (d) a plate/slide holding stage controlled in the Y direction.

source, a macro zoom lens (TS-93005, SUGITOH), and a CCD image sensor (DFK23U618, Imaging Source) placed above the print head chamber. The chamber was filled with 3T3 suspension with DPBS solution, and the signal with several frequency components was applied to the piezoelectric actuator for observation.

2.5. Evaluation of Cell Ejection Stability

To evaluate ejection stability, NIH/3T3 cell suspensions were fluorescently labeled with Cell Tracker Green (Thermo Fisher Scientific Inc.) and diluted in DPBS at determined densities before being loaded into the inkjet printhead chamber. Ejecting mode signals and mixing mode signals as defined above were applied alternately at intervals of 500 ms, which allowed the deposition of droplets at a frequency of 2 Hz. The droplets were deposited onto glass slides fixed to an automated moving stage so that the number of cells in each droplet could be counted after printing under a fluorescence microscope (Axio observer D1, Carl Zweiss).

2.6. Cell Viability Assay After Ejection

NIH/3T3 or HUVEC cell suspensions were prepared at concentrations of 1×10^6 cells/ml in DPBS. 30 µL of the cell suspension was loaded into the inkjet head chamber. The cells were ejected for about 30 min with a droplet ejection frequency of 100 Hz into a microcentrifuge tube containing 1 ml of the appropriate culture medium and then counted and dispensed into a 96-well culture plate at a density of 3×10^3 cells per well. Cell ejection experiments were conducted in triplicate. As control samples, the initial cell suspensions before ejection were manually dispensed into a 96-well culture plate using a 100 µL micropipette. The plates were placed in a 5% CO_2 incubator at 37.0°C until measurement. Apoptotic and necrotic cells were quantified in each well using the Apoptotic/Necrotic cell detection kit (Promokine, PromoCell GmbH) according to the instructions of the manufacturer. The stained cultures were observed under a fluorescence microscope (Axio observer D1, Carl Zeiss), and images were taken so that between 200 and 500 cells could be analyzed for each sample. Early apoptotic cells were identified on the basis of green fluorescent staining (FITC-Annexin V) of their plasma membranes and necrotic cells based on red fluorescent staining (EthD-III) of their nuclei. Double positive cells exhibiting both green and red fluorescent staining were considered late apoptotic cells. The total number of cells was determined by counting all the nuclei stained in blue by Hoechst 33342.

2.7. Cell Proliferation Assay

The cell suspensions were ejected into a microcentrifuge tube for the cell viability assay and dispensed into a 96-well culture plate at a density of 3×10^3 cells per well. The WST-1 colorimetric assay (Premix WST-1Cell Proliferation Assay System, Takara Bio Inc.) was used to evaluate the proportion of actively metabolizing live cells in each well. Measurements were performed in triplicate using three wells at each time point. 10 µL of the WST-1 reaction solution was added to each well containing the cells and 100 µL culture medium. The plates were returned to the 5% CO_2 incubator for 1 h and incubated at 37.0°C. Absorbance at 420 nm was measured using a plate reader (Cytation 5, BioTek Instruments, Inc.). The measured data were normalized relative to the measurements obtained 4 h post-ejection.

2.8. Embryonic Stem Cell Clonogenic Assay and Immunostaining

Mouse embryonic stem cells (mES cells, Merck) were maintained in gelatin-coated dishes with feeder cells (Merck) as recommended by the manufacturer. The cells were detached using Accutase (Merck), centrifuged at 100 g for 5 min at 4°C, and suspended in DPBS through a 20 µm filter to make bioinks. After ejection, the cells

were seeded at a density of 2.5×10^4 cell/well in 24-well plates and cultured for 3 days. The average numbers of colony-forming units were counted after staining with red alkaline phosphatase substrate kit (VECTOR laboratories). For immunostaining, the cells were fixed with 4% paraformaldehyde and incubated overnight at 4°C with primary antibodies, Nanog (abcam) 1:200, SSEA-1 (abcam) 1:100, 2 h at room temperature with secondary antibodies, and 5 min with 1:10,000 Hoechst 33342 (Thermo Fisher Scientific).

2.9. 3D Bioprinting System Setup

A bioprinting system has been designed as shown in Figure 1B for constructing 3D tissues with multiple cell types. The present system is equipped with newly developed cell-printing inkjet heads and commercial industrial inkjet heads for ejecting biomaterials. A maximum of three cell-printing inkjet heads can be mounted in parallel so that three types of cells can be printed sequentially to develop tissues with heterogeneous patterns. The position of the nozzle is controlled horizontally on the X-axis and vertically on the Z-axis to allow the deposition of cells not only for surface patterning but also in three dimensions. In addition, two industrial multi-nozzle inkjet heads (MH2420 Print Head, Ricoh) allow the successive printing of two different liquids such as a hydrogel precursor and an appropriate cross-linking reagent, enabling the formation of fast-gelling layers over a large area. The industrial heads can also be controlled independently on the X- and Z-axis. The stage is controlled on the Y-axis and can hold glass slides at the back and culture plates at the front.

2.10. 2D Drop-on-demand Patterning Evaluation

To evaluate the control of droplet deposition using two cell-printing heads in a sequential manner, two separate suspensions of NIH/3T3 cells were prepared at a concentration of 3×10^6 cells/ml in DPBS. To distinguish between the suspensions, the cells were fluorescently labeled with CellTracker Green or Orange (Thermo Fisher Scientific Inc.) according to the instructions of the manufacturer. Cell-containing droplets were deposited with a sinusoidal waveform and an ejection frequency of 50 Hz onto a glass slide. Phase-contrast and fluorescent microscopy images were taken using a laser scanning confocal microscope (FV10i, Olympus Corporation).

2.11. 3D Multilayering Evaluation

For 3D constructs, the general process for developing multilayered structures with alternating cell and hydrogel deposition is described in Figure 2 in section 3. Four separate bioinks were prepared as follows: 0.5 wt% sodium alginate as scaffold bioink 1; 100 mM calcium chloride ($CaCl_2$) as scaffold bioink 2; 5×10^7 cells/ml NHDF cells stained with Cell Tracker Green and suspended in DPBS and 0.5 wt% sodium alginate as cell-laden bioink 1; and 5×10^7 cells/ml NHDF cells stained with Cell Tracker Orange and suspended in DPBS and 0.5 wt% sodium alginate as cell-laden bioink 2. Printing was performed on a glass slide as follows: (a) A layer of sodium alginate was deposited by ejecting scaffold bioink 1 using the first industrial head at 10 Hz, immediately followed by (b) a layer of $CaCl_2$ using the second industrial head for rapid gelling of a thin alginate hydrogel scaffold layer; (c) cell-laden bioink 1 was deposited with a cell-printing printhead at 10 Hz to draw a 10 mm line along the X-axis; (d) a hydrogel scaffold layer was superimposed onto the cell layer using the same procedure in (a) and (b); and (e) the cell-laden bioink 2 was deposited with a cell-printing printhead at 10 Hz to draw a 10 mm line along the Y-axis. The steps from (a) to (e) were repeated until a 10-layer construct was achieved. To observe the superposition of layers, cross-sectional Z-stack images of the multilayered constructs were acquired using a confocal laser scanning microscope (TCS SP8 STED CW, Leica Microsystems) at the intersection of the green and orange cell lines after fixation in ethanol.

3. Results

3.1. Inkjet Printhead Design

Ejecting living cell suspensions using inkjet technology generally presents several challenges. Figure 3A illustrates a simplified representation of a common piezoelectric inkjet printhead and summarizes the three most notable issues when using such a device. First, the typical cell size is 100 times larger than typical pigments in printing ink solutions so that nozzle and channel clogging occurs as cells rapidly sink to the bottom. Cell sedimentation also makes it a challenge to obtain a stable number of cells per droplet since the density inside the chamber is not maintained at a homogeneous state. Second, air bubbles are trapped in the cell suspension due to high surface tension, which negatively affects the reliability of droplet ejection. Third, a cell suspension with a large volume is required to fill up the entire chamber and enable the piezoelectric actuator induce liquid pressure for droplet ejection.

Therefore, here, we have developed a novel printhead optimized for live cell-printing (cell-printing head) that could replace conventional printheads. As shown in Figure 3B, the cell-printing head is composed of an open chamber where the cells are directly loaded, a disc-shaped membrane fixed at the circumference of the bottom of the chamber, a nozzle with an aperture at the center of the

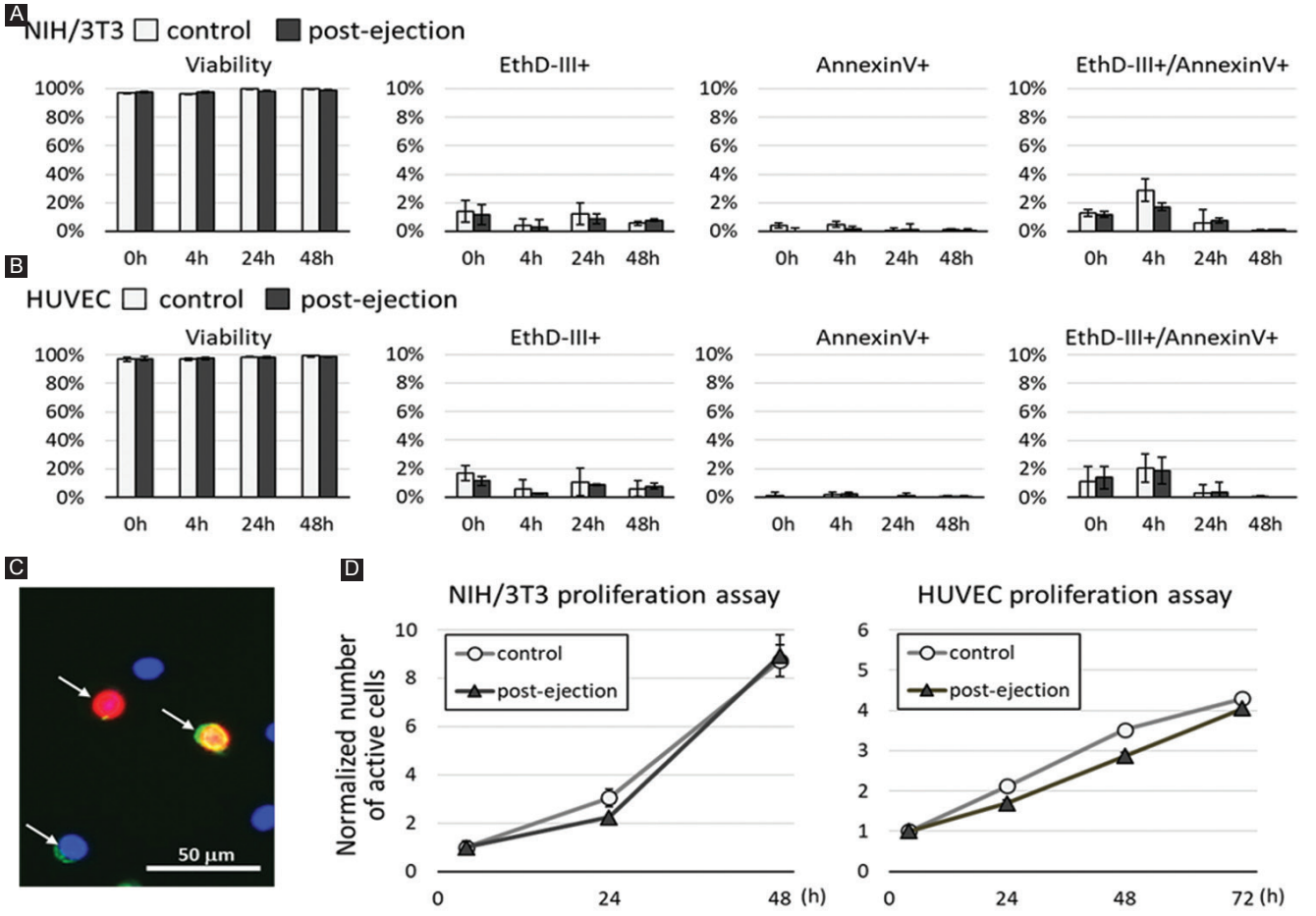

Figure 2. Analysis of cell survival after ejection from the new inkjet head. (**A**) Percentages of unstained viable cells, EthD-III positive (necrotic) cells, FITC-Annexin V positive (apoptotic) cells, and double positive (late apoptotic) cells in NIH/3T3 cell cultures from 0 to 48 h post-ejection compared with control cultures seeded by manual pipetting. Error bars show the standard deviations of triplicate cultures with 200-500 cells analyzed per sample. (**B**) Same as (**A**) for human umbilical blood vein endothelial cell (HUVEC) cultures. (**C**) Representative fluorescence microscopy image of NIH/3T3 cells stained using the Apoptotic/Necrotic cell detection kit. White arrows indicate the three different types of stained cells: Red cells for EthD-III, green cells for FITC-Annexin V, and double positive yellow cells. All cell nuclei are stained blue with Hoechst 33342. Scale bar: 50 µm. (**D**) Quantification of active live cells in NIH/3T3 and HUVEC in WST-1 proliferation assay. The data were normalized and reported as a ratio relative to the measurement at 4 h.

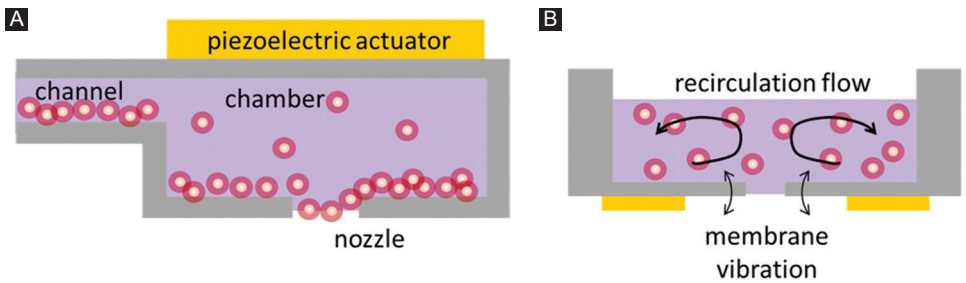

Figure 3. Schematic diagram of a cross-sectional view of inkjet heads. (**A**) Common printhead showing nozzle clogging with the sedimentation of cells. (**B**) Cell-printing head, with a recirculation flow generated by membrane vibration to prevent nozzle clogging.

membrane, and an annular piezoelectric actuator fixed on the outer side of the membrane. The advantages of the cell-printing head are that first, as illustrated in Figure 3B, membrane movements driven by the piezoelectric actuator can establish a recirculating flow inside the chamber to prevent cell sedimentation. Second, air bubbles trapped during droplet ejection can be easily evacuated from the open side. Third, the cell-printing head can be loaded

with volumes as low as a few dozen microliters without compromising droplet formation.

3.2. Evaluation of Inkjetting Condition

To determine the optimal printing conditions, optical monitoring devices were assembled as follows. Observation of drop formation was carried out, as illustrated in Figure 4A. By applying a signal as shown in Figure 4B to the piezoelectric actuator of the cell-printing head, a droplet is ejected from the cell-printing head. Frequency of the applied signal was fixed to the fundamental frequency of the membrane.

Results of drop formation with voltage amplitudes between 4.4 and 5.8 V are shown in Figure 4C. One drop formation is achieved when the voltage V ranges from 4.8 to 5.4 V. When the voltage is lower than 4.8 V, the pressure required for drop formation cannot be achieved. Conversely, when the voltage is higher than 5.4 V, minute droplets (mist and satellite) are formed.

A droplet forming process in the cell printhead will be described with reference to the schematic view as shown in Figure 4E and F. When the membrane is displaced from the original state to the liquid chamber side and suddenly pushes the liquid; pressure is generated at the interface between the membrane and liquid. Since the pressure is easily released into the atmosphere through the nozzle rather than through the upper aperture of the chamber or pushes back the membrane, the meniscus protrudes out of the nozzle (Figure 4E). Thereafter, the membrane attempts to revert to the original position. However, if the liquid in the nozzle portion at the time receives an adequate velocity, the liquid droplet is considered to be formed, as shown in Figure 4F.

3.3. Evaluation of Mixing Condition

Observation of cell suspension mixing was carried out as illustrated in Figure 5A, and the signal is shown in Figure 5B with several frequencies applied to the piezoelectric actuator for the observation.

The circle in each figure indicates the membrane. The nozzle is located in the center of the membrane, and ring-shaped mirror images of the illuminations are seen in each figure. In Figure 5C, uniform mixing mode is observed by applying the signal at a frequency near the fundamental frequency of the membrane (20 kHz). Conversely, the periodic pattern is observed by applying a

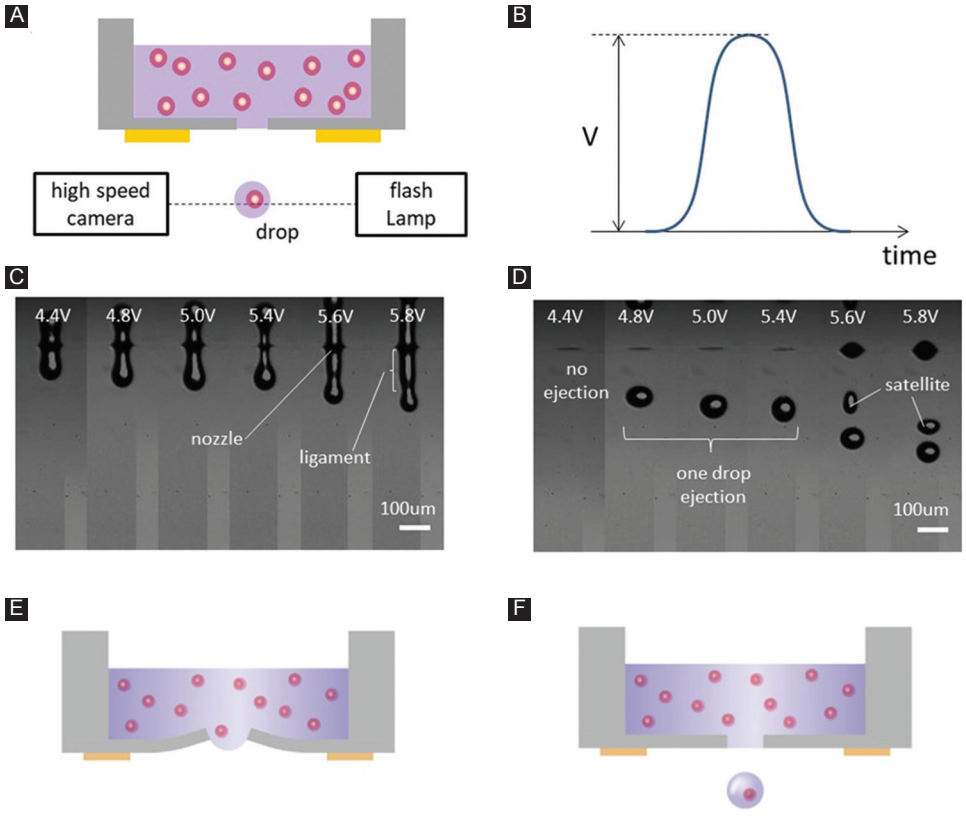

Figure 4. Observation of droplet formation from the cell printhead. (**A**) Observing mechanism of droplet formation using a high-speed camera and a flash lamp. (**B**) Addition of sine curve signals to piezoelectric actuator. (**C**) Observation of droplet after 200 µs, addition of 4.4, 4.8, 5.0, 5.4, 5.6, and 5.8 V and compare each droplet formation. (**D**) Observation of droplet after 316 µs, one drop ejection with 4.8, 5.0, and 5.4 V. (**E**) Schematic diagram of droplet formation in 200 µs. (**F**) Schematic diagram of droplet forming in 316 µs.

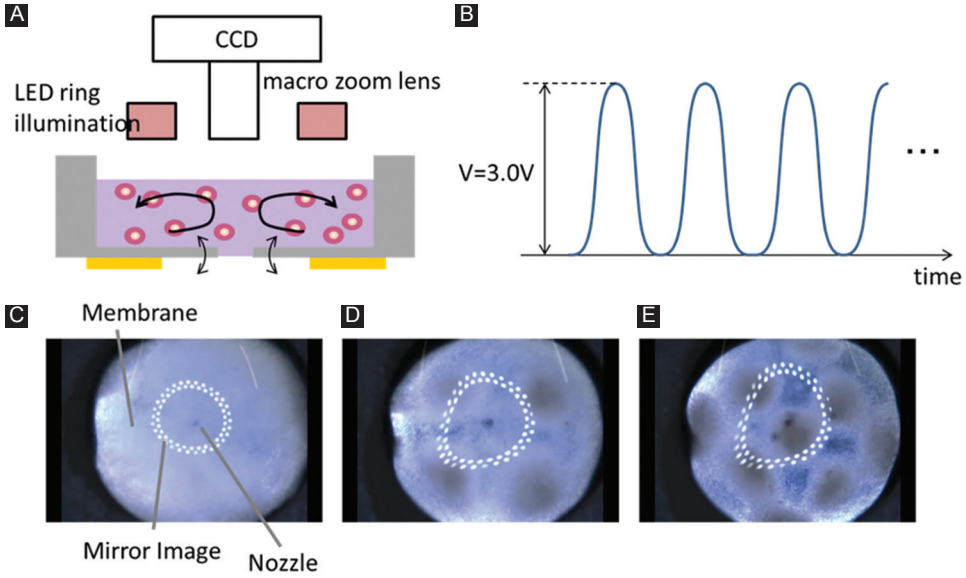

Figure 5. Observation of mixing cell suspension in the chamber. (**A**) Mixing status is checked by CCD, a micro zoom lens, and ring illumination. (**B**) For mixing cell suspension, a sinusoidal signal was applied with a fixed amplitude of 3.0 V. (**C**) Mixing status with the fundamental frequency of the membrane, 20 kHz. (**D**) and (**E**) Mixing mode with higher-order vibration mode, 72.0 and 74.0 kHz.

higher frequency such as 72.0 kHz. 74.0 kHz is applied in Figure 5D and E. The phenomena are expected to induce higher-order vibration modes. At such a higher-order vibration mode, the antinodes and nodes of vibration are generated, and cells gathering into the node position were observed, as shown in Figure 5D and E. Therefore, the preferred signal frequency for mixing cells is not one of a higher-order vibration mode of the membrane but one near the fundamental mode.

Appropriate single cell droplet formation was achieved when a single peak sinusoidal signal was applied to the piezoelectric actuator with a voltage amplitude between 4.8 and 5.4 V (ejecting mode), whereas uniform mixing was achieved when the signal had a frequency close to the fundamental frequency of the vibrating membrane at a fixed amplitude of 3 V (mixing mode).

3.4. Evaluation of Ejection Stability

Developing bioprinted tissue at any substantial volume or amount, as required in applications such as organ regeneration or drug screening, would require a reliable deposition of cell-containing droplets over a considerable period. Therefore, maintaining a stable number of cells per droplet for an adequately long time is critical in inkjet bioprinting. Optimization of the signals applied to the piezoelectric actuator to enable the use of the cell-printing head is described in section 2.2. Briefly, a single peak sinusoidal signal with a voltage amplitude between 4.8 and 5.4 V (ejecting mode) allows a single cell-containing droplet to be ejected by the movement of the membrane at the nozzle. Drop-on-demand ejection, therefore, can be achieved by controlling the signal applied to the printhead. Between each ejection, a weak sinusoidal vibration is applied to the membrane to maintain the cells in suspension (mixing mode). Alternating the ejecting mode and mixing mode signals at fixed time intervals allows the deposition of droplets at a constant frequency. The results for the evaluation of ejection stability are shown in Figure 6A. Droplets were ejected at a frequency of 2 Hz using cell suspensions at three different cell densities and were ejected without mixing mode as a reference. The number of cells per droplet was stable for over 15 min at any of the tested cell densities with mixing mode. Conversely, unstable ejecting was observed with the reference sample. At 0 min, the same cell number was observed with mixing and without mixing; however, average cell number increased with the lapse of time. The observations indicate that mixing mode could be ejected with stable cell number. The graph in Figure 6B illustrates the average cell number and the standard deviation with mixing mode samples calculated over the entire length of the 15 min ejection experiment. The average number of cells per droplet had a linear relationship with the initial density of cell suspension, which suggests that the number of cells per droplet can be adjusted by selecting the appropriate cell density when preparing the bioink cell suspension. Here, using a bioink with a cell density of 3×10^6 cells/ml would allow the deposition of around 1.5 cells per droplet on average. This indicates that high accuracy control of cell number in each droplet is achieved using the cell-printing head.

In addition, the histograms in Figure 7 show that the number of cells per droplet at 0 and 15 min is consistent with a Poisson distribution profile at any of the tested cell

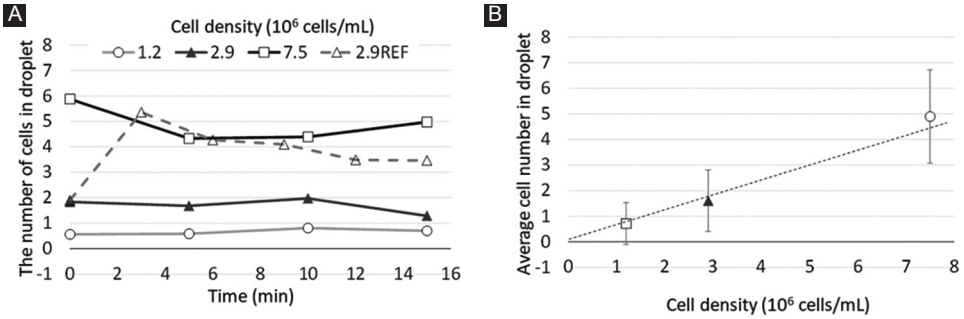

Figure 6. Evaluation of ejection stability. Droplets of cell suspensions were ejected at a frequency of 2 Hz onto a glass slide. Then, the cell number in each droplet was counted under a fluorescence microscope. (**A**) Average cell count per droplet for the three initial cell densities: 1.2E + 06, 2.9E + 06, and 7.5E + 06 cells/mL. As a reference, 2.9E + 06 cells/ml were ejected without mixing mode. (**B**) Average cell number in droplet are plotted with each cell density. Error bar is 1 sigma.

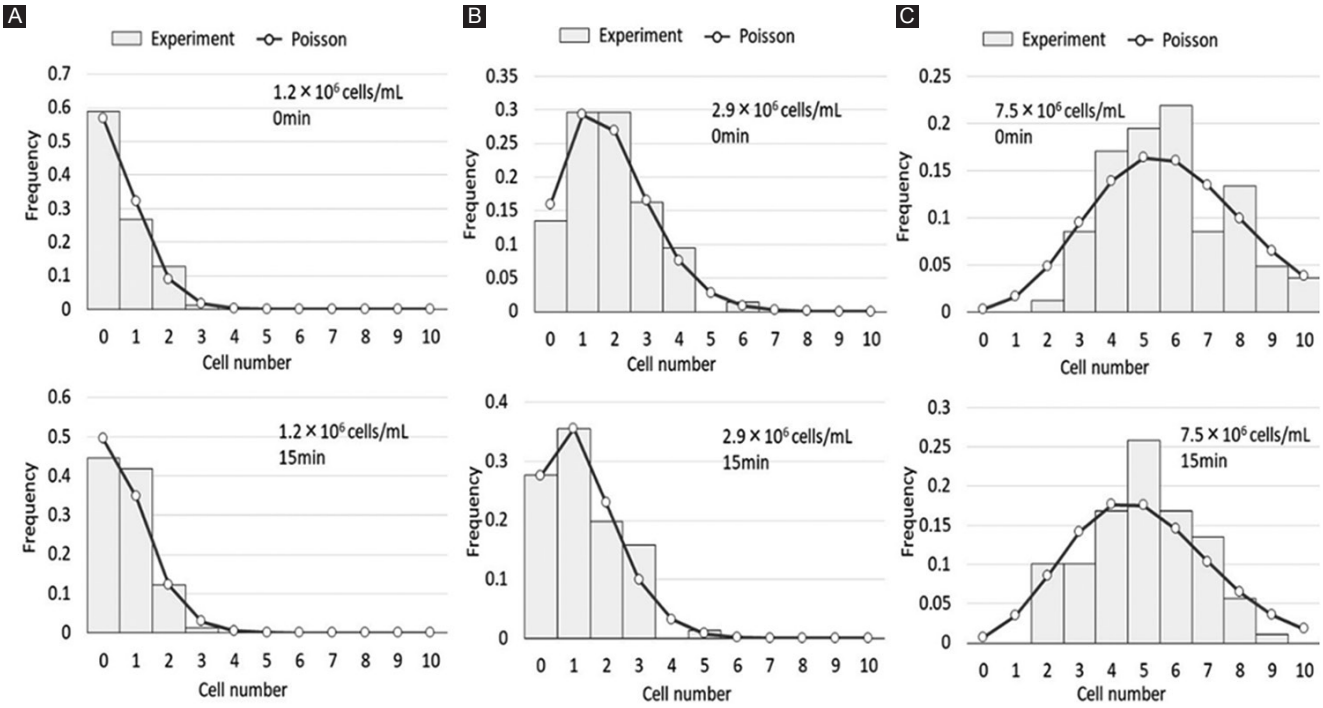

Figure 7. Histogram plot of cell number in each droplet. (**A**) Result with 1.2E + 06 cells/ml in 0 and 15 min. Dot is value with the Poisson distribution. The blue bar is experimental value. (**B**) Result with 2.9E + 06 cells/mL. (**C**) Result with 7.5E + 06 cells/mL.

densities. The observation indicates that the cells inside the head chamber were maintained in suspension with a random distribution for a long time, which confirms that the mixing mode of the cell-printing head achieved its function.

3.5. Cell Viability and Proliferation after Ejection

Cell viability was evaluated at 0, 4, 24, and 48 h after ejection into the culture medium. Printing was carried out with the voltage previously applied but with the droplet ejection frequency increased to 100 Hz to enable the collecting of a higher number of cells. The cells were ejected into the culture medium for 30 min and then aliquoted into a 96-well plate and placed in a 5% CO_2 incubator at 37.0°C. The cultures were then fluorescently stained with FITC-Annexin V to identify early apoptotic cells in green and with Ethidium Homodimer III (EthD-III) to identify necrotic cells in red. The percentages of each cell type relative to the total number of cells analyzed post-ejection were compared with those of control cultures seeded by manual pipetting.

As shown in Figure 2, very high viability of between 97% and 99% was demonstrated for NIH/3T3 and HUVEC after printing. No significant difference was observed compared with the control cultures, either for apoptotic cells or for necrotic cells. The WST-1 proliferation assay revealed

that despite a slight decrease at 24 h in NIH/3T3 cells and between 24 and 48 h for HUVEC, the post-ejection samples recovered normally and achieved a proliferation rate similar to that of the manually seeded controls after 48-72 h. To further assess functional recovery in a more sensitive type of cells, a similar experiment was performed using mES cells, as shown in Figure 8. No significant effect was observed on the clonogenic ability and the expression of stem cell markers in mES cells cultured for 3 days after ejection. Overall, the results demonstrate that using our newly developed inkjet printhead does not significantly affect cell viability and functionality, at least for the cell types used in the present study.

3.6. Precise Drop-on-demand Live Cell Patterning

A novel inkjet bioprinting system has been developed as described in Figure 1B of section 2 to demonstrate the feasibility of multi-ink live cell deposition. Our bioprinter is equipped with three of the novel cell-printing heads described previously, which allow handling of up to three independent cell suspensions simultaneously.

Drop-on-demand control of cell deposition was evaluated by ejecting a predefined number of droplets of cell suspensions onto a glass slide. Figure 9A shows the results using two different suspensions of fibroblast cells at a density of 3×10^6 cells/ml, one labeled with fluorescent cell tracker green and the other with cell tracker orange, with a distance of 500 µm between the dots. The previous results for ejection stability showed that when using a suspension with an initial density of 3×10^6 cells/mL, about 1.5 cell count per droplet can be expected on average. Here, two droplets were deposited per dot, which allowed the observation of an average of three cell counts per dot.

In addition, the ability to control cell number with variable droplets was assessed, as shown in Figure 9B. The average number of cells per deposition exhibited a linear relationship with the number of ejected droplets, which suggests that the number of cells per deposition can be adjusted by selecting the appropriate number of droplets. This indicates that high accuracy control of cell number in each deposition is also achieved with the cell-printing head.

3.7. Biofabrication Process for the Development of 3D Mille-Feuille-like Constructs

A multilayering process for constructing 3D tissues was developed, as described in Figure 10. In addition to being equipped with cell-printing heads, our inkjet bioprinting prototype has two industrial multi-nozzle heads, which allow rapid deposition of two liquid materials such as precursors of hydrogel scaffolds into thin layers.

By alternating hydrogel scaffold layers made of sodium alginate deposition, followed immediately by $CaCl_2$ ion cross-linking, and fluorescently labeled cell suspension layers, Mille-Feuille-like bicolor constructs could be produced, as reported in Figure 11A. Cross-section images along the vertical Z-axis acquired under confocal laser scanning microscopy revealed that the finely stratified multilayer structure was well preserved. As reported in the example of Figure 11B, it was also demonstrated that the distance between each cell layer could be controlled by increasing the number of steps during the deposition of hydrogel scaffold layers.

4. Discussion

The newly developed inkjet printhead introduced in the present study has been particularly optimized for live cell bioprinting. The unique features of the cell-printing head allow the controlled ejection of single droplets on demand while maintaining the cells in suspension inside the printhead chamber. The analysis of the number of cells per droplet revealed that a stable ejection could be maintained for dozens of minutes of continuous printing, which is a significant improvement over conventional piezoelectric printheads. Notably, achieving a consistent cell count per droplet and, more preferably, approaching a state where a single cell is contained in each droplet

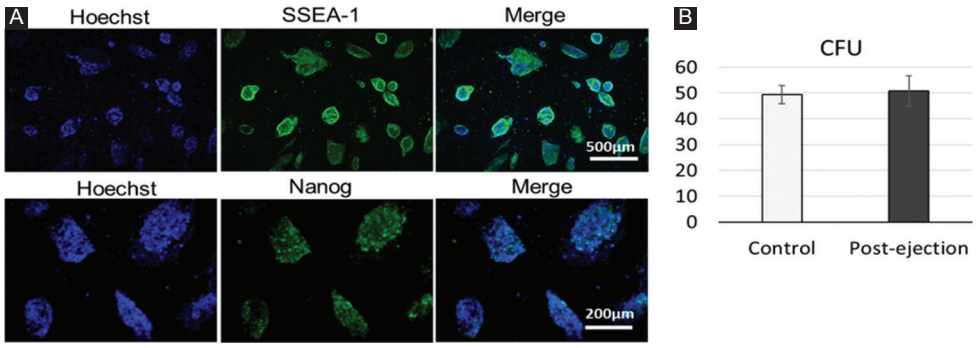

Figure 8. Analysis of mouse embryonic stem (mES) cell clonogenic cell survival. (**A**) Immunostaining of mES colonies with stem cell markers. (**B**) Average number of colony-forming unit counted at day 3 of culture after seeding by manual pipetting (control) or by inkjet (post-ejection). Error bars show the standard deviations of four microscopic images.

would be a major step toward the modeling of highly detailed 3D structures at the resolution of a single cell. The results showed that the new cell-printing head could eject cells with a cell per droplet consistent with the Poisson distribution profile, which indicated that the cell suspension was maintained in a well-homogenized state by the mixing system.

However, to achieve an even narrower distribution and further increase the precision of deposition, it would be necessary to bring the state of random distribution closer to a state of uniform distribution for the cells in suspension inside the printhead chamber. This would require a strong repulsive force that acts between the cells, so that they are not brought close to each other, for example, by introducing a polymer with a charge polarity that could provide an electrostatic repulsive force between the cells. We are also investigating the potential of employing additional optical cell count systems to further control the number of cells per droplet.

Regarding the suitability of using the new printheads with living cells, analysis of cell viability and proliferation revealed that the ejected cells were not significantly affected, even following the application of sensitive cells such as undifferentiated stem cells. In contrast to a previous report evaluating cell injury during laser bioprinting[19], no marked increase in necrotic nor in apoptotic cells was observed from 0 to 48 h. The results are potentially because the level of stress induced by our current process is lower than that in laser printing. The cells recovered and proliferated normally after inkjet printing and were expected to maintain the integrity of their functions, including the clonogenicity of stem cells.

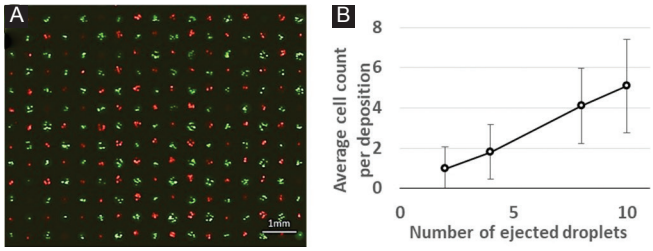

Figure 9. Drop-on-demand two-dimensional patterning evaluation (**A**) Fluorescence microscope image of green- and red-labeled NIH/3T3 cells deposited alternately at 500 μm intervals with two cell-containing droplets ejected at each position. (**B**) Ability to control the number of cells based on the number of ejected droplets. Cell ink was formulated to contain one cell in two droplets. Error bars show the standard deviations.

Our printheads bear several features are considerably different from common industrial inkjet heads and could minimize cell damage. The open chamber structure and the mixing system allow use over extended periods without compromising gaseous exchange, whereas rapidly evacuating bubbles before their accumulation increases the risk of damage following rupture[20]. The simplicity of the printhead chamber architecture and the use of membrane vibration for droplet generation avert any excessive increase in liquid pressure and shear stress before ejection. Further investigations are required to assess the physical mechanisms that negatively influence cell viability and function the most.

It is also worth noting, from a practical point of view, particularly considering potential biomedical applications that the printhead chamber was intentionally kept simple to ensure that low volumes of cell suspensions could be loaded easily. Simplifying the procedures for loading and exchanging cell suspensions could further reduce the risks of environmental stress and contamination. This could also be a major advantage when using rare cells that are difficult to expand since our system does not require filling ink cartridges or wasting cell suspensions for maintenance.

Achieving a reliable ejection of living cells allowed us to subsequently experiment with more advanced processes for the spatial positioning of cell-containing droplets. We have demonstrated that an on-demand patterning of cells over a flat surface is feasible with precise control of cell number at each deposition. Most notably, the potential to draw intricate patterns with arrays

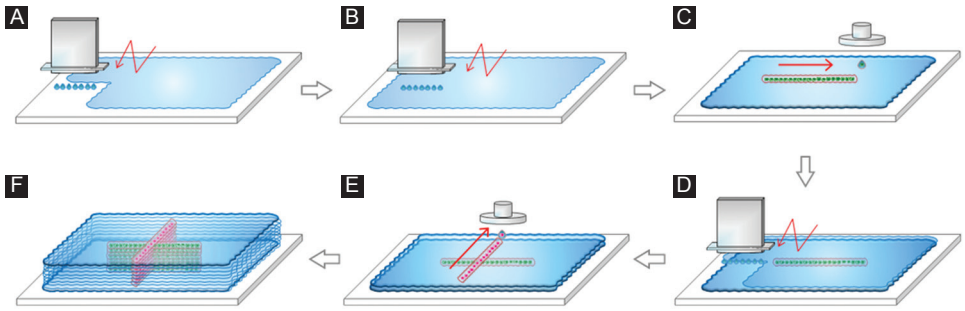

Figure 10. Schematic of three-dimensional inkjet cell-printing process. (**A**) Printing of a scaffold hydrogel precursor before gelation. (**B**) Printing of gelation factor. (**C**) Printing of the first cell ink. (**D**) A hydrogel scaffold layer is superimposed onto the cell layer by the same procedure in (**A**) and (**B**). (**E**) Printing of the second cell ink. (**F**) The steps from (**A**) to (**E**) are repeated until a multilayer construct is achieved.

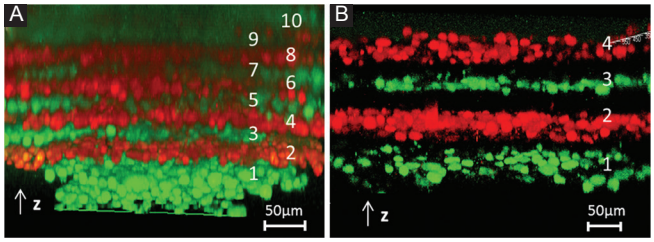

Figure 11. Confocal fluorescence microscope Z-stack images of multilayered Mille-Feuille-like three-dimensional cellular constructs. (**A**) Ten-layer constructs made by the alternate printing of green and red fluorescently labeled fibroblasts with alginate hydrogel scaffold layers deposited in between. (**B**) Four-layer constructs with distances between each cell layer increased by the deposition of thicker hydrogel layers.

of multiple cell types and density gradients is a promising feature of inkjet bioprinting that would be unmatched by other methods. Bicolor arrays have been successfully printed in the present study to test the principle, and even more complex pattern designs could be achieved should the need arise. Our unique combination of cell-printing printheads and industrial printheads also allowed us to develop multilayered structures by association with hydrogel biomaterials, with a controlled thickness down to only a dozen micrometers between each layer. Various strategies for layer-by-layer cell deposition have been attempted previously[21,22]; however, to the best of our knowledge, this is the first report of such finely stratified cellular constructs developed entirely based on an inkjet system. One ultimate goal would be to achieve true drop-on-demand printing at single-cell resolution, which would signal the potential for novel approaches for the reconstruction and exploration of the complexity of tissue microenvironments in synergy with the recent rapid advances in single cell analysis.

Despite considerable progress, our technology still faces several limitations that are yet to be resolved. The first issue is that the X-Y surface printing resolution decreases when attempting to draw continuous lines or to increase the density of cellular deposition. Our lines are generally around 100 µm wide, which can be considered quite thick compared with the high resolution we have achieved on the vertical Z direction. This is essentially due to physical properties such as surface tension of the printed materials that can result in the cells moving away from the droplet impact point before their immobilization. Therefore, further optimization and validation are required by taking into account variable cell size, cell density, and materials used as bioink. Finally, the development of bioink materials is also crucial for improving tissue construction in 3D. To obtain fully functional tissues, hydrogel materials that hold the cells together should not only provide physical support but also be biocompatible and able to promote appropriate cellular growth and maturation[23]. In this regard, our method requires fast-gelling materials with rheological properties that are compatible with a stable ejection from the inkjet printhead while ensuring precise deposition and rapid immobilization of cells into layers. We are currently using alginate hydrogel as the material of choice since both its precursor and its cross-linking agent (calcium chloride) can be inkjet-printed and provide adequate mechanical strength by forming a solid scaffold layer on contact. However, alginate is not often appropriate for long-term culture since it lacks the cell-adhesive properties required for the cells to interact and function properly[17]. Investigations on more suitable materials are underway to provide cellular environments closer to native ECM, including the use of modified alginate, or blending with other cell-adhesive and biodegradable polymers such as fibrin and gelatin[24].

5. Conclusions

The present study demonstrates that inkjet bioprinting has the potential to become one of the most powerful technologies for precise tissue construction. Our experience in industrial printing allowed us to address each challenge with systematic engineering solutions. First, an innovative printhead specifically designed to eject living cell suspensions has been developed, and the printing conditions have been optimized for reliable dispensing and cell survival. In addition, a multi-ink bioprinting system has been built to demonstrate that cells and materials can be effectively arranged in both 2D high-precision patterns and 3D multilayered constructs in a unique manner. Mechanical refinements and biomaterial development are still required to improve patterning resolution and 3D tissue formation. However, inkjet bioprinting could evolve into a versatile system for the production of structurally organized multicomponent constructs tailored to meet the requirements of various applications such as regenerative medicine, *in vitro* testing, or disease modeling.

Acknowledgment

We thank Naoki Satoh, Yuzuru Kuramochi, and Satoshi Nakazawa for their technical assistance and the Ricoh Material Analysis Technology Research Department for help in taking confocal images.

Authors' Contributions

M.S. and D.T. supervised the project and designed the original inkjet device and printing system. W.L., T.M., H.Y., and S.H. designed the experiments. T.M., H.Y., and N.H. conducted the experiments. W.L. and T.M. analyzed the data. D.T. wrote the manuscript. All authors reviewed the manuscript.

Conflicts of Interest

The authors are employees of the sponsor of this study. However, this did not influence the objectivity of the study. The authors declare that they do not have any competing interests.

References

1. Takahashi K, Tanabe K, Ohnuki M, *et al*., 2007, Induction of Pluripotent Stem Cells from Adult Human Fibroblasts by Defined Factors. *Cell,* 131(5):861-72. DOI 10.1016/j.cell.2007.11.019.
2. Groll J, Boland T, Blunk T, *et al*., 2016, Biofabrication: Reappraising the Definition in an Evolving Field. *Biofabrication,* 8(1):13001-6. DOI 10.1088/1758-5090/8/1/013001.
3. Murphy SV, Atala A, 2014, 3D Bioprinting of Tissues and Organs. *Nat Biotechnol*, 32(8):773-85. DOI 10.1038/nbt.2958.
4. Arslan-Yildiz A, El Assal R, Chen P, *et al*., 2016, Towards Artificial Tissue Models: Past, Present, and Future of 3D Bioprinting. *Biofabrication,* 8(1):14103. DOI 10.1088/1758-5090/8/1/014103.
5. Gudupati H, Dey M, Ozbolat I, 2016, A Comprehensive Review on Droplet-based Bioprinting: Past, Present and Future. *Biomaterials,* 102:20-42. DOI 10.1016/j.biomaterials.2016.06.012.
6. Derby B, 2008, Bioprinting: Inkjet Printing Proteins and Hybrid Cell-containing Materials and Structures. *J Mater Chem*, 18(47):5717-21. DOI 10.1039/b807560c.
7. Xu T, Jin J, Gregory C, *et al*., 2005, Inkjet Printing of Viable Mammalian Cells. *Biomaterials,* 26(1):93-9. DOI 10.1016/j.biomaterials.2004.04.011.
8. Nakamura M, Kobayashi A, Takagi F, *et al*., 2005, Biocompatible Inkjet Printing Technique for Designed Seeding of Individual Living Cells. *Tissue Eng*, 11(11-12):1658-66. DOI 10.1089/ten.2005.11.1658.
9. Saunders RE, Gough JE, Derby B, 2008, Delivery of Human Fibroblast Cells by Piezoelectric Drop-on-demand Inkjet Printing. *Biomaterials,* 29(2):193-203. DOI 10.1016/j.biomaterials.2007.09.032.
10. Gross A, Schöndube J, Niekrawitz S, *et al*., 2013, Single-cell Printer: Automated, on Demand, and Label Free. *J Lab Autom*, 18(6):504-18. DOI 10.1177/2211068213497204.
11. Cheng E, Yu H, Ahmadi A, *et al*., 2016, Investigation of the Hydrodynamic Response of Cells in Drop on Demand Piezoelectric Inkjet Nozzles. *Biofabrication,* 8(1):15008. DOI 10.1088/1758-5090/8/1/015008.
12. Herran CL, Huang Y, Chai W, 2012, Performance Evaluation of Bipolar and Tripolar Excitations During Nozzle-jetting-based Alginate Microsphere Fabrication. *J Micromech Microeng,* 22(8):85025. DOI 10.1088/0960-1317/22/8/085025.
13. Kim YK, Park JA, Yoon WH, *et al*., 2016, Drop-on-demand Inkjet-based Cell Printing with 30-μm Nozzle Diameter for Cell-level Accuracy. *Biomicrofluidics,* 10(6):064110. DOI 10.1063/1.4968845.
14. Arai K, Iwanaga S, Toda H, *et al*., 2011, Three-dimensional Inkjet Biofabrication Based on Designed Images. *Biofabrication,* 3(3):34113. DOI 10.1088/1758-5082/3/3/034113.
15. Cui X, Boland T, 2009, Human Microvasculature Fabrication using Thermal Inkjet Printing Technology. *Biomaterials,* 30(31):6221-7. DOI 10.1016/j.biomaterials.2009.07.056.
16. Faulkner-Jones A, Fyfe C, Cornelissen DJ, *et al*., 2015, Bioprinting of Human Pluripotent Stem Cells and their Directed Differentiation into Hepatocyte-like Cells for the Generation of Mini-livers in 3D. *Biofabrication,* 7(4):44102. DOI 10.1088/1758-5090/7/4/044102.
17. Nakamura M, Iwanaga S, Henmi C, *et al*., 2010, Biomatrices and Biomaterials for Future Developments of Bioprinting and Biofabrication. *Biofabrication,* 2(1):14110. DOI 10.1088/1758-5082/2/1/014110.
18. Perçin G, Khuri-Yakub BT, 2003, Piezoelectric Droplet Ejector for Ink-jet Printing of Fluids and Solid Particles. *Rev Sci Instrum*, 74(2):1120-7. DOI 10.1063/1.1532839.
19. Zhang Z, Chai W, Xiong R, *et al*., 2017, Printing-induced Cell Injury Evaluation During Laser Printing of 3T3 Mouse Fibroblasts. *Biofabrication,* 9(2):25038. DOI 10.1088/1758-5090/aa6ed9.
20. Hu W, Berdugo C, Chalmers JJ, 2011, The Potential of Hydrodynamic Damage to Animal Cells of Industrial Relevance: Current Understanding. *Cytotechnology,* 63(5):445-60. DOI 10.1007/s10616-011-9368-3.
21. Moon S, Hasan SK, Song YS, *et al*., 2010, Layer by Layer Three-dimensional Tissue Epitaxy by Cell-laden Hydrogel Droplets. *Tissue Eng Part C Methods,* 16(1):157-66. DOI 10.1089/ten.tec.2009.0179.
22. Koch L, Deiwick A, Schlie S, *et al*., 2012, Skin Tissue Generation by Laser Cell Printing. *Biotechnol Bioeng,* 109(7):1855-63.
23. Malda J, Visser J, Melchels FP, *et al*., 2013, 25th Anniversary Article: Engineering Hydrogels for Biofabrication. *Adv Mater,* 25(36):5011-28. DOI 10.1002/adma.201302042.
24. Jungst T, Smolan W, Schacht K, *et al*., 2016, Strategies and Molecular Design Criteria for 3D Printable Hydrogels. *Chem Rev,* 116(3):1496-539. DOI 10.1021/acs.chemrev.5b00303.